Journal of Water Process Engineering 5 (2015) 95–100

Contents lists available at ScienceDirect

Journal of Water Process Engineering

journal homepage: www.elsevier.com/locate/jwpe

Short communication

New facile benign agrogenic-nanoscale titania material—Remediation potential for toxic inorganic cations

Martins O. Omorogie[a,c,*], Jonathan O. Babalola[b], Emmanuel I. Unuabonah[c,d], Jian R. Gong[a,**]

[a] Laboratory for Nanodevices, National Center for Nanoscience and Technology–Chinese Academy of Sciences (NCNST–CAS), 100190 Beijing, People's Republic of China
[b] Biophysical Chemistry Unit, Department of Chemistry, University of Ibadan, 200284 Ibadan, Nigeria
[c] Environmental and Chemical Processes Research Laboratory, Department of Chemical Sciences, Redeemer's University, P.M.B. 3005, Mowe, Ogun State 110115, Nigeria
[d] Institüt fur Chimie, Universität Potsdam, D-14476, Germany

ARTICLE INFO

Article history:
Received 3 September 2014
Received in revised form 9 January 2015
Accepted 14 January 2015

Keywords:
Biomass
Kinetics
Agrogenic-nanoscale titania
Chromium
Lead

ABSTRACT

A new facile benign (eco-friendly) *Nauclea diderrichii* agrowaste-nanoscale titania hybrid adsorbent (TND) used in the sequestration of Cr(III) and Pb(II) ions is reported in this paper. Surface characterization techniques such as thermogravimetric analysis (TG), X-ray diffractometry (XRD), scanning electron microscopy (SEM), transmission electron microscopy (TEM) and Brunauer–Emmett–Teller (BET) surface area and porosimetric analyses indicated that *N. diderrichii* agrowaste (NDS) was successfully modified with nano-titania. TG analysis proved that modification of *N. diderrichii* agrowaste with nano-titania improved its thermal stability and rate of metal ion uptake. Pseudo-second order kinetic equation gave better fit to experimental data than pseudo-first order kinetic equation. The adsorption capacity of NDS and TND adsorbents for Cr(III) were 5.57 mg/g and 6.21 mg/g, respectively. Also, the amounts of Pb(II) sequestered by NDS and TND adsorbents were 6.82 mg/g and 7.49 mg/g, respectively. Also, the initial sorption rates of Cr(III) and Pb(II) by TND adsorbent was higher than for NDS adsorbent, making TND material a better adsorbent for toxic metal ions removal from aqueous effluents than NDS adsorbent.

1. Introduction

Global industrialization has led to the release of toxic metal ions into the environment. Moreover, industrialization and urbanization have resulted in an elevation of the amounts of toxic metal ions present in the natural habitat, which comprises soils, lakes, rivers, ground-waters and oceans, thereby causing environmental pollution [1,2].

Environmental pollution from toxic metal ions (Ni(II), Cu(II), Cd(II), Cr(III) and Pb(II)) occurs in different industrial wastewaters, which are metal plating, mining operations, metallurgical engineering, battery manufacturing processes, production of paints and pigments, electroplating, nuclear power plants, ceramic industries and glass industries [3–6]. These toxic metal ions are deleterious to the ecosystem [1,2]. Their non-biodegradable nature allows them bio-accumulate in living organisms, thereby posing precarious health challenges for the entire flora, fauna and human beings [6].

A long time exposure to Cr(III) species can cause skin allergies, cancer and DNA damage in human beings [7]. Lead is a known carcinogen and its bioaccumulation in living organisms causes disruption in the biosynthesis of the haemoglobin level, a rise in blood pressure, kidney damage in human beings, and then brain damage, miscarriages, abortions and diminished learning abilities of children [3–6].

The removal of these hazardous metal ions from water and wastewaters is essential for protecting human health and the ecosystem. The quest to remove these toxic metal ions from the environment has led to the use of various separation techniques. Metal ion uptake by biosorption may involve the contribution of diffusion, adsorption, chelation, complexation, and coordination or micro-precipitation mechanisms depending on the specificity of the biosorbent. The utilization of nanoscale materials has the merit

* Corresponding author at: Environmental and Chemical Processes Research Laboratory, Department of Chemical Sciences, Redeemer's University, P.M.B. 23005, Mowe, Ogun State 110115, Nigeria. Tel.: +234 802 682 7920.
** Corresponding author. Tel.: +86 10 82545649.
E-mail addresses: osaigbovoohireimen@gmail.com (M.O. Omorogie), gongjr@nanoctr.cn (J.R. Gong).

http://dx.doi.org/10.1016/j.jwpe.2015.01.003
2214-7144/

of increasing the surface areas of biosorbents, and thus increasing their biosorptive applications [8].

Over the years, vast studies have been carried out on the adsorption of hazardous metal ions by different waste materials of biological origin such as sugarcane bagasse [9], waste orange peel [10], wheat bran [11], rice bran [12], Japanese cedars [13], *Thuja orientalis* [14], reed [15], *Carica papaya* [16,17], *Nauclea diderrichii* [18,19], clay [20], fly ash, guar gum-nano zinc oxide [21,22], natural clinoptilolite [23], Ca-alginate beads [24], lime fly ashes [25], bacteria exopolymer, gall nut, oak fruit [26], *Trichoderma harzianum* [27], *Anthrobacter* sp. biomass [28], *Zea mays* seed chaff [29], mesoporous silica and graphene oxide nanoparticles-modified *N. diderrichii* [30,31], biomass-derived fly ash [32], etc. The effects of these hazardous metal ions on the environment are fast growing and thus researchers have shown keen interest in using materials of biological origin (agrolignocellulosics) to develop selective adsorbents to combat this global menace [3].

Two major drawbacks of adsorbents of agricultural origin are that they easily degrade (bleed) in solutions after few hours and they are unable to withstand high temperatures during use [33]. These limit their industrial application. An attempt to overcome these challenges has been demonstrated by Unuabonah et al. [33,34] who made a *C. papaya*-kaolinite clay combo adsorbent with high efficiency for the removal of metal ions from aqueous solutions.

This study reports the development, characterization and application of a new facile environmentally-benign adsorbent prepared from *N. diderrichii* agrolignocellulosic waste (NDS) and nano-titania for the removal of Cr(III) and Pb(II) ions from aqueous solutions. The NDS-nano titania hybrid adsorbent (TND) prepared is expected to have high adsorption capacity and initial sorption rate for the toxic metal ions when compared with NDS. TND is reported for the first time to sequester Cr(III) and Pb(II) ions from aqua system.

2. Materials and methods

2.1. Preparation of NDS, nano-titania and TND

N. diderrichii seeds were obtained from the Forest Research Institute of Nigeria (FRIN), in Ibadan (7° 23′ 16″ North, 3° 53′ 47″ East), Nigeria. After collection, it was heated in an oven at 60 °C for 3 h. Thereafter, it was pulverized and sieved to 450 μm particle size.

Nano-titania was synthesized using the sol–gel method by Choi et al. [35]. Transparent colloidal particles were formed immediately, which after evaporation led to a yellowish titania powder. This as-prepared yellowish titania powder was calcined at 550 °C for 6 h until the amorphous and low crystalline titania powder metamorphosed into highly crystalline titania powder.

Thereafter, the yellowish titania powder and NDS were placed in a 1 L beaker containing 700 mL ultra-pure de-ionized water from millipore water instrument in the ratio 0.5–1. The reaction mixture was agitated at 1000 rpm at 20 °C for 48 h. The NDS-nano titania hybrid adsorbent (TND) was also filtered by vacuum filtration and the wet TND material was placed in a heating crucible and dried at 100 °C overnight. The TND material was weighed into 3 mL plastic containers and kept for use in adsorption study.

2.2. Characterizations of NDS, nano-titania and TND

N. diderrichii seed agrolignocellulosic (NDS), nano-titania and TND were characterized using PerkinElmer Fourier Transform Infra Red (FTIR) spectrometer, Micromeritics Instrument Corporation, ASAP 2020 Model Analyzer (for Brunauer–Emmett–Teller (BET) nitrogen sorption–desorption multi-point analysis at 77 K), X-ray diffractometer (XRD) (D/Max-2500, Rigaku, Japan) with Cu Kα radiation, PerkinElmer thermogravimetric analyzer (TG), F20 S-TWIN transmission electron microscope (TEM) (Tecnai G2, FEI Co.) and scanning electron microscope (SEM) (Hitachi S4800 Model).

2.3. Adsorption study

Fifty milligrams of NDS and TND adsorbents each were added to 20 mL of 20 mg/L of Cr(III) and Pb(II) aqueous solutions, prepared from $Cr(NO_3)_3{\cdot}9H_2O$ and $Pb(NO_3)_2$ salts, both of analytical grade, whose pH values were adjusted to 7.0 and 5.0, respectively, (pH values of maximum adsorption obtained from initial pH study {data not shown}) with either 0.1 M HNO_3 or NaOH.

For kinetic study, the suspensions under the same conditions above were agitated between 5 and 60 min, at 125 rpm and at temperatures of 303 K in a thermostatic shaker. Samples were withdrawn at various time intervals and filtered using filter papers. The supernatants obtained were analyzed for residual Cr(III) and Pb(II) ions using ICP-OES (inductively coupled plasma-optical emission spectrometer), PerkinElmer Optima 5300 DV Model. The amounts of Cr(III) and Pb(II) sequestered by NDS and TND adsorbents were calculated by difference using the equation;

$$q_e = \frac{(C_o - C_e)V}{W} \tag{1}$$

where C_o is the initial concentration of metal ion (mg/L), C_e is the equilibrium concentration of residual metal ion in the solution (mg/L), V is the volume of the aqueous solution containing metal ions (L), W is the weight of adsorbent (g) and q_e is the amount of metal ion adsorbed by the adsorbent (mg/g).

Experimental data obtained from thermodynamic and kinetic studies described above were fitted into pseudo-second order [36], pseudo-first order [37], diffusion–chemisorption [38,39] and Weber–Morris intraparticle diffusion [18,40] models, respectively, which are written mathematically as:

$$\frac{t}{q_t} = \frac{t}{q_e} + \frac{1}{k_2 q_e^2} \tag{2}$$

$$h_{\text{ads}} = k_2 q_e^2 \tag{3}$$

$$\ln(q_e - q_t) = \ln q_e - k_1 t \tag{4}$$

$$\frac{t^{0.5}}{q_t} = \frac{t^{0.5}}{q_e} + \frac{1}{K_{\text{DC}}} \tag{5}$$

$$q_t = K_{\text{ip}} t^{1/2} + \psi \tag{6}$$

where $k_1, k_2, h_{\text{ads}}, q_t, K_{\text{ip}}, \psi, K_{\text{DC}}$ are pseudo-first order rate constant (/min), pseudo-second order rate constant (g/mg min), initial sorption rate (mg/g min), amount of metal ion adsorbed at time t(min) by the adsorbent (mg/g), Weber–Morris intraparticle diffusion constant (mg/g $\text{min}^{1/2}$), the value film layer thickness and rate of mass transfer of adsorbate (mg/g $t^{1/2}$), respectively.

3. Results and discussion

3.1. FTIR analyses of NDS, nano-titania and TND

The FTIR spectrum of NDS has been previously described by Omorogie et al. [19]. Fig. 1 shows the FTIR spectra of nano-titania and TND. The FTIR spectrum of nano-titania showed a long shoulder peak at 1092 cm^{-1} and short peaks at 3291 cm^{-1}, 2926 cm^{-1}, 1619 cm^{-1} and 801 cm^{-1} indicating —C—O stretch vibration from titania precursor (titanium isopropoxide), surface —O—H stretch, —C—H stretch vibration due to titania precursor, —C=O stretch vibration and —C—O in-plane deformation for Ti—O, respectively [41]. For TND, the surface —O—H stretch at 3291 cm^{-1} in nano-titania became broadened and shifted to 3432 cm^{-1}. This may due to the modification of nano-titania with NDS. Also, various

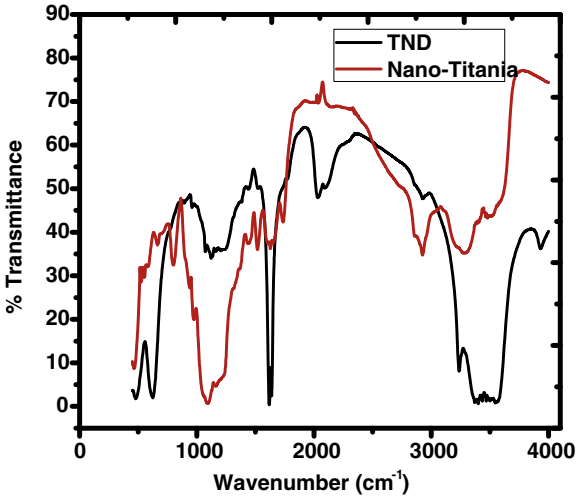

Fig. 1. FTIR spectra of nano-titania and TND.

peaks were observable at 3237 cm^{-1}, 1609 cm^{-1}, 1128 cm^{-1} and 625 cm^{-1} represent —C—H stretch vibration, —C=O stretch vibration, —C—O stretch vibration and —C—O in-plane deformational vibration, respectively [41,42].

3.2. TG, XRD, SEM, TEM and BET analyses of NDS, nano-titania and TND

The thermogravimetric analysis (TG) of NDS adsorbent (Fig. 2a) has been described in our previous work [18]. The TG thermogram for nano-titania (Fig. 2a) indicated that there was weight loss between 20 and 200 °C (ca. 2%). This was due to loss of surface water, ethanol and concentrated HNO_3. Thereafter, there was no further weight loss. Similar results were obtained for TND adsorbent. However, between 200 and 550 °C, TND adsorbent showed a weight loss of ca. 20% as a result of loss of lignins and cellulosics [6,42]. It is interesting to note that a weight loss between 600 and 1000 °C (ca. 50%) observed for NDS [18] was not observed in TND adsorbent suggesting that the TND adsorbent is more thermally stable than NDS adsorbent. Also, the nano-titania used for the modification of NDS adsorbent was non-degradable between 600 and 1000 °C, and thus eliminated the weight loss of NDS adsorbent at this temperature range. Nano-titania is known for its high thermal stability at high temperatures. This thermo-stable property of TND adsorbent gives it an edge in industrial application over NDS adsorbent.

The XRD pattern of NDS (Fig. 2b) was described in our previous work [19]. Nano-titania showed a peak intensity around Bragg angle $2\theta = 27°$. Other small peak intensities were shown at Bragg angles $2\theta = 25°$, 37°, 42°, 57.5°, which are (1 0 1), (0 0 4), (2 0 0), (2 1 1) reflection peaks, respectively. These are typical of anatase nano-titania polymorph [43]. A broad peak at $2\theta = 69°$ and a medium peak intensity $2\theta = 54.5°$ were observed for TND adsorbent (Fig. 2b). This signified that the diffraction peaks at $2\theta = 42°$ and 57.5° for nano-titania shifted to $2\theta = 54.5°$ and $2\theta = 69°$ for TND adsorbent due to the addition of nano-titania to NDS adsorbent.

The SEM image of NDS adsorbent was described in our previous work [18]. The SEM image of TND adsorbent showed particles that are unevenly dispersed (Fig. 3a and b). The SEM images of nano-titania showed flat but very tiny particles.

The BET surface area and pore width of NDS adsorbent increased from 5.36 to 6.54 m^2/g and 3.01 to 6.88 nm, respectively, on modification with nano-titania. Also, the Barrett–Joyner–Halenda (BJH) adsorption cumulative surface area of pores and adsorption cumulative volume of pores for NDS adsorbent increased from 6.34 to 7.66 m^2/g and 0.00632 to 0.00945 cm^3/g, respectively, when it was modified with nano-titania (see Table 1).

Moreover, there was an increase in the single point surface area of NDS at relative pressure (P/P_o) from 2.53 to 7.41 m^2/g after modification with nano-titania. It is also interesting to note that the average pore width of NDS adsorbent after modification with nano-titania (TND adsorbent) was greater than those of NDS adsorbent and nano-titania. The reason for this was owing to the fact that nano-titania modifier was responsible for the increase in the BET/BJH surface areas and pore widths of NDS adsorbent, due to its possession of better BET/BJH surface areas and pore widths. The nitrogen sorption–desorption plots for NDS adsorbent at 77 K has been reported by Omorogie et al. [19]. Fig. 3c and d show the nitrogen sorption–desorption plots for nano-titania and TND adsorbent at 77 K, and Fig. 3e shows the pore width distribution curves for nano-titania, TND and NDS adsorbents.

The TEM image of nano-titania indicated the presence nanoparticles that are visible between 100 and 200 nm (Fig. 3f).

3.3. Kinetic data analysis

Adsorption kinetics is very significant in analyzing experimental data obtained from adsorption study. It gives information about the mechanism of the adsorbate onto the adsorbent which is critical

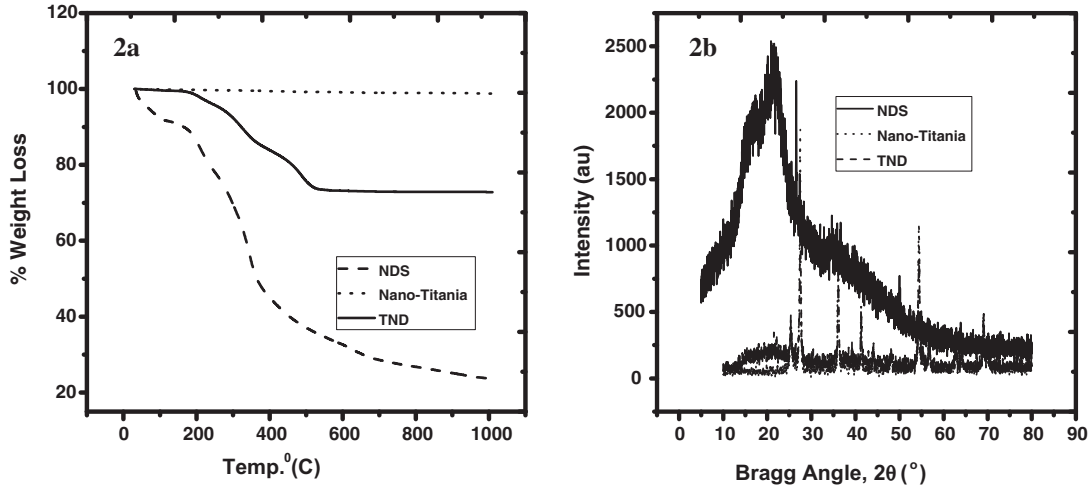

Fig. 2. (a) TG thermograms, (b) XRD patterns of NDS, nano-titania and TND.

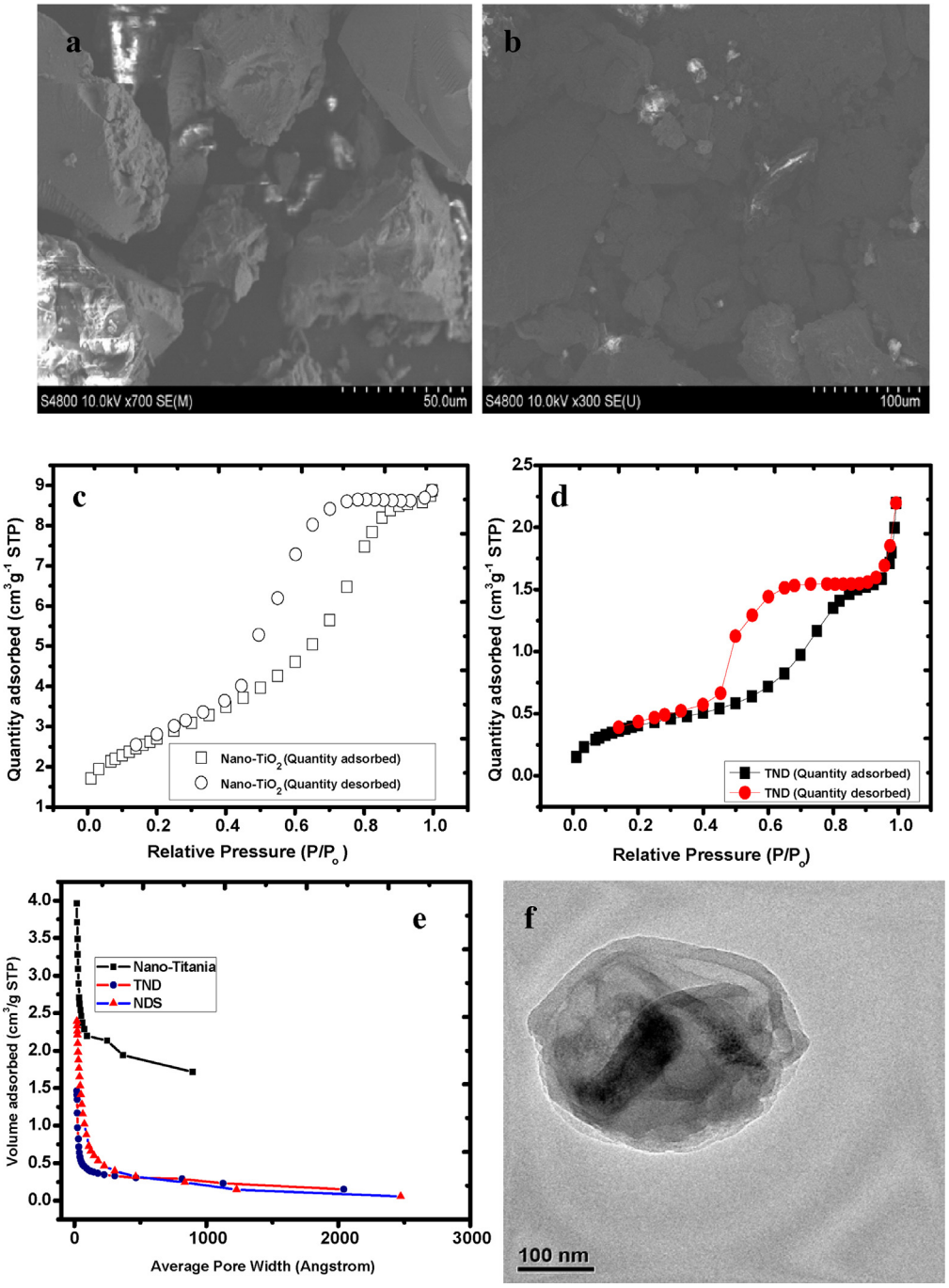

Fig. 3. SEM images of (a) nano-titania and (b) TND, BET Nitrogen sorption–desorption plots of (c) nano-titania and (d) TND at 77 K, (e) Pore width distribution curves for nano-titania, TND and NDS, and (f) TEM image of nano-titania.

Table 1
Multi-point surface parameters from nitrogen sorption–desorption at 77 K for nano-titania, NDS and TND.

	Single point surface area at P/P_o (m^2/g)	BET surface area (m^2/g)	T-plot external surface area (m^2/g)	BJH adsorption cumulative surface area of pores (m^2/g)	Single point adsorption total pore volume of pores (cm^3/g)	BJH adsorption cumulative volume of pores (cm^3/g)	BET adsorption average pore width (nm)	BJH adsorption average pore width (nm)
Nano-titania	9.424	9.786	9.651	10.219	0.0135	0.0141	5.531	5.529
NDS	2.532	5.357	7.454	6.341	0.00404	0.00632	3.014	3.985
TND	7.410	6.543	8.684	7.657	0.00865	0.00945	6.875	8.352

Data were obtained from Omorogie et al. [31].

Table 2
Kinetic parameters for the sequestration of Cr(III) and Pb(II) onto NDS and TND.

	NDS		TND	
	Cr(III)	Pb(II)	Cr(III)	Pb(II)
Pseudo-first order				
q_e (mg/g)	0.650	0.170	1.208	1.043
k_1 (/min)	0.050	0.060	0.010	0.013
R^2	0.837	0.985	0.839	0.814
Pseudo-second order				
q_e (mg/g)	5.570	6.210	6.820	7.490
k_2 (g/mg min)	0.230	1.610	0.301	0.322
h_{ads} (mg/g min)	7.140	62.090	14.085	188.050
R^2	0.999	1.000	1.000	1.000
Diffusion-chemisorption				
q_e (mg/g)	5.590	6.220	6.200	7.040
$K_D K_{DC}$ (mg/g $t^{1/2}$)	29.940	196.080	32.210	49.650
R^2	0.998	1.000	0.996	0.998
Weber-Morris intraparticle diffusion				
K_{ip} (mg/g $min^{1/2}$)	2.007	2.391	2.172	2.565
Ψ	0.375	0.556	0.497	0.525
R^2	0.891	0.824	0.843	0.867

Table 3
Adsorption capacities of some adsorbents for Cr(III) and Pb(II) ions.

Adsorbent	Adsorbent dose (g/L)	Initial metal conc.	Adsorption capacity (mg/g)
Cr^{3+} **			
Plataneus orientalis leaves	2.0	≤40 mg/L	5.01
Plant ulmus leaves	2.0	≤40 mg/L	0.9–5.0
Lignocellulosic peat	1.0	≤200 mg/L	0.16
Rosa damascena phytomass	0.1	100 mg/L	140.0
Sugarcane bagasse	4.0	≤1000 mg/L	13.4
This study (NDS)	2.5	20 mg/L	5.57
This study (TND)	2.5	20 mg/L	6.82
Pb^{2+} ***			
Nizimuddinia zanardini	2.0	0.5 mmol/L	50.41
Padina australis	2.0	0.5 mmol/L	46.51
Sargassum glaucescens	2.0	0.5 mmol/L	45.84
Cystoseira indica	2.0	0.5 mmol/L	47.22
$CaCl_2$-coated Padina australis	2.0	0.5 mmol/L	48.25
This study (NDS)	2.5	20 mg/L	6.21
This study (TND)	2.5	20 mg/L	7.49

** Cr^{3+}: extracted from Sen and Dastidar, [45] and Ullah et al. [46].
*** Pb^{2+}: extracted from Montazer-Rahmati et al. [42].

to its practical application. Experimental data obtained were fitted with four kinetic models: pseudo-second order, pseudo-first order, diffusion-chemisorption and Weber-Morris intraparticle diffusion kinetic models. Among the kinetic models used, pseudo-second order kinetic model provided the best fit to experimental data. It was observed from Table 2 that the amounts of Cr(III) and Pb(II) adsorbed, q_e, by NDS adsorbent were 5.57 mg/g and 6.21 mg/g, respectively, and the amounts of Cr(III) and Pb(II) adsorbed, q_e, by TND adsorbent were 6.82 and 7.49 mg/g, respectively. Table 2 also showed that the initial sorption rates, h_{ads} (g/mg min) for the sequestration of Cr(III) and Pb(II) by TND adsorbent were higher than those of NDS adsorbent. This lucidly indicates that the doping of NDS with nano-titania was responsible for TND's higher adsorption capacity. Cr(III) and Pb(II) adsorbed by TND adsorbed was 85.25% and 93.625%, respectively, compared with that of NDS adsorbent, which were 69.625% and 77.625%, respectively. Slight increase in the surface area and pore width of NDS, and the interstitial spacing of nano-titania [43] used to modify NDS may also be responsible for the increase in the uptake of Cr(III) and Pb(II) ions onto TND adsorbent. Weber-Morris intraparticle diffusion model showed that all the values of $\psi > 0$. This implies that intraparticle diffusion was not the only rate-determining step for the adsorption process. Film or pore diffusion might also be involved in the rate-determining step of this process [44].

Furthermore, Table 3 shows the adsorption capacities of some adsorbents in literature for Cr(III) and Pb(II) ions, compared with those of NDS and TND adsorbents.

4. Conclusion

A comparison of the sequestration of Cr(III) and Pb(II) by *N. diderrichii* agrowaste and TND adsorbents were reported in this study. TND adsorbent gave better adsorption capacities for Cr(III) and Pb(II) than *N. diderrichii* agrowaste. From thermo-gravimetric analysis, the modification of *N. diderrichii* agrowaste with nano-titania improved its thermal stability (anti-degradable property), as well as increasing its adsorption capacities and uptake rates of toxic metal ions studied. This enhances the potential use of nano-titania modified *N. diderrichii* agrowaste and indeed other agrowaste modified with nano-titania for water treatment on industrial scale.

Acknowledgements

The authors acknowledge the support of The World Academy of Sciences for the advancement of science in developing countries (TWAS), Italy and the Chinese Academy of Sciences (CAS), China for providing Fellowship (FR number: 3240240234) to Dr Martins O. Omorogie at the Laboratory for Nanodevices of the National Center for Nanoscience and Technology, Beijing, China where this research was done. This work was also partly supported by the National Basic Research Program of China (973 Program No. 2011CB933401) and the National Natural Science Foundation of China (21005023). Professor Jian R. Gong gratefully acknowledges the support of the K.C. Wong Education Foundation, Hong Kong.

References

[1] M. Ahmaruzzaman, V.K. Gupta, Rice husk and its ash as low-cost adsorbents in water and wastewater treatment, Ind. Eng. Chem. Res. 50 (2011) 13589–13613.
[2] A. Mudhoo, V.K. Garg, S. Wang, Removal of heavy metals by biosorption, Environ. Chem. Lett. 10 (2012) 109–117.
[3] H. Li, W. Shi, H. Shao, M. Shao, The remediation of the lead-polluted garden soil by natural zeolite, J. Hazard. Mater. 169 (2009) 1106–1111.
[4] W. Shi, H. Shao, H. Li, M. Shao, S. Du, Progress in the remediation of hazardous heavy metal-polluted soils by natural zeolite, J. Hazard. Mater. 170 (2009) 1–6.
[5] M. Nadeema, A. Mahmooda, S.A. Shahid, S.S. Shah, A.M. Khalid, G. McKay, Sorption of lead from aqueous solution by chemically modified carbon adsorbents, J. Hazard. Mater. B 138 (2006) 604–613.
[6] M.E. Argun, S. Dursun, G.M. Karatas, Activation of pine cone using fenton oxidation for Cd(II) and Pb(II) removal, Bioresour. Technol. 99 (2008) 8691–8698.
[7] Y.S. Yun, D. Park, J.M. Park, B. Volesky, Biosorption of trivalent chromium on the brown seaweed biomass, Environ. Sci. Technol. 35 (2001) 4353–4358.
[8] S. Baytak, F. Zereen, Z. Arslan, Preconcentration of trace elements from water samples on a minicolumn of yeast (*Yamadazyma spartinae*) immobilized TiO_2 nanoparticles for determination by ICP-AES, Talanta 84 (2011) 319–323.
[9] D.C. Sharma, C.F. Forster, A preliminary examination into the adsorption of hexavalent chromium using low-cost adsorbents, Bioresour. Technol. 47 (1994) 257–264.
[10] C. Namasivayam, N. Muniasamy, K. Gayathri, M. Rani, M. Ranganathan, Removal of dyes from aqueous solutions by cellulosic waste orange peel, Bioresour. Technol. 57 (1996) 37–43.
[11] L. Dupont, E. Guillon, Removal of hexavalent chromium with a lignocellulosic substrate extracted from wheat bran, Environ. Sci. Technol. 37 (2003) 4235–4241.
[12] K.K. Singh, R. Rastogi, S.H. Hasan, Removal of Cr(VI) from wastewater using rice bran, J. Colloid Interface Sci. 290 (2005) 61–68.
[13] M. Aoyama, M. Kishino, T.-S. Jo, Biosorption of Cr(VI) on Japanese cedar bark, Sep. Sci. Technol. 39 (2005) 1149–1162.
[14] E. Oguz, Adsorption characteristics and the kinetics of the Cr(VI) on the *Thuja oriantalis*, Colloids Surf. A Physicochem. Eng. Aspects 252 (2005) 121–128.

[15] Z. Rawajfih, N. Nsour, Thermodynamic analysis of sorption isotherms of chromium(VI) anionic species on reed biomass, J. Chem. Thermodyn. 40 (2008) 846–851.
[16] E.I. Unuabonah, G.U. Adie, L.O. Onah, O.G. Adeyemi, Multistage optimization of the adsorption of methylene blue dye onto defatted *Carica papaya* seeds, Chem. Eng. J. 155 (2009) 567–579.
[17] G.U. Adie, E.I. Unuabonah, A.A. Adeyemo, O.G. Adeyemi, Biosorptive removal of Pb^{2+} and Cd^{2+} onto novel biosorbent: defatted *Carica papaya* seeds, Biomass Bioenergy 35 (7) (2011) 2517–2525.
[18] M.O. Omorogie, J.O. Babalola, E.I. Unuabonah, J.R. Gong, Kinetics and thermodynamics of heavy metal ions sequestration onto novel *Nauclea diderrichii* seed biomass, Bioresour. Technol. 118 (2012 a) 576–579.
[19] M.O. Omorogie, J.O. Babalola, E.I. Unuabonah, W. Song, J.R. Gong, Efficient chromium abstraction from aqueous solution using a low-cost biosorbent: *Nauclea diderrichii* seed waste, J. Saudi Chem. Soc. (2012) (In press) http://dx.doi.org/10.1016/j.jscs.2012.09.017
[20] T.A. Khan, V.V. Singh, Removal of cadmium(II), lead(II), and chromium(VI) ions from aqueous solution using clay, Toxicol. Environ. Chem. 92 (8) (2010) 1435–1446.
[21] T.A. Khan, V. Singh, I. Ali, Sorption of Cd(II), Pb(II), and Cr(VI) metal ions from wastewater using bottom fly ash as low cost sorbent, J. Environ. Prot. Sci. 3 (2009) 124–132.
[22] T.A. Khan, M. Nazir, I. Ali, A. Kumar, Removal of chromium(VI) from aqueous solution using guar gum–nano zinc oxide biocomposite adsorbent, Arabian J. Chem. (2013) (In press) http://dx.doi.org/10.1016/j.arabjc.2013.08.019
[23] N. Beyazit, Batch and column studies on zinc removal from industrial wastewater using natural clinoptilolite: factors affecting sorption capacities and kinetics, Toxicol. Environ. Chem. 95 (1) (2013) 45–68.
[24] Y.-L. Lai, M. Thirumavalavana, J.-F. Lee, Effective adsorption of heavy metal ions (Cu^{2+}, Pb^{2+}, Zn^{2+}) from aqueous solution by immobilization of adsorbents on Ca-alginate beads, Toxicol. Environ. Chem. 92 (4) (2010) 697–705.
[25] A.A.B. Moghala, P.V. Sivapullaiah, Retention characteristics of Cu^{2+}, Pb^{2+} and Zn^{2+} from aqueous solutions by two types of low lime fly ashes, Toxicol. Environ. Chem. 92 (10) (2012) 1941–1953.
[26] A.M. Latifi, S.M. Nabavi, M. Mirzaei, M. Tavalaei, H. Ghafuriand, C. Hellio, S.F. Nabavi, Bioremediation of toxic metals mercury and cesium using three types of biosorbent: bacterial exopolymer, gall nut, and oak fruit particles, Toxicol. Environ. Chem. 92 (9) (2012) 1670–1677.
[27] M.N. Zafar, A. Wahid, M.A. Ghauri, M. Zubair, M.W. Mumtaz, F. Anwar, M. Danisha, Trichoderma harzianum: a green sorbent for Pb(II) uptake from aqueous solutions, Toxicol. Environ. Chem. 95 (3) (2013) 422–433.
[28] K.S. Prasad, A.L. Ramanathan, J. Paul, V. Subramanian, R. Prasad, Biosorption of arsenite (As^{+3}) and arsenate (As^{+5}) from aqueous solution by *Arthrobacter* sp. biomass, Environ. Technol. 34 (19) (2013) 2701–2708.
[29] J.O. Babalola, M.O. Omorogie, A.A. Babarinde, E.I. Unuabonah, V.O. Oninla, Optimization of the biosorption of Cr^{3+}, Cd^{2+} and Pb^{2+} using a new biowaste: *Zea mays* seed chaff, Environ. Eng. Manage J. (2013) (In press) http://omicron.ch.tuiasi.ro/EEMJ/pdfs/accepted/367_153_Babalola_12pdf
[30] M.O. Omorogie, J.O. Babalola, E.I. Unuabonah, J.R. Gong, Solid phase extraction of hazardous metals from aqua system by nanoparticle-modified agrowaste composite adsorbents, J. Environ. Chem. Eng. 2 (1) (2014) 675–684.
[31] M.O. Omorogie, J.O. Babalola, E.I. Unuabonah, J.R. Gong, Hybrid materials from agrowaste and nanoparticles: implications on the kinetics of the adsorption of inorganic pollutants, Environ. Technol. 35 (5) (2014) 611–619.
[32] U. Vaid, S. Mittal, J.N. Babu, Removal of hexavalent chromium from aqueous solution using biomass derived fly ash from waste-to-energy power plant, Desalin. Water Treat. (2013) (In press) http://dx.doi.org/10.1080/19443994.2013.833554
[33] E.I. Unuabonah, C. Gunter, J. Weber, S. Lubahn, A. Taubert, Hybrid clay: a new highly efficient adsorbent for water treatment, ACS Sustain. Chem. Eng. 1 (8) (2013) 966–973.
[34] E.I. Unuabonah, A.O. Adedapo, C.O. Nnamdi, A. Adewuyi, M.O. Omorogie, K.O. Adebowale, B.I. Olu-Owolabi, A.E. Ofomaja, A. Taubert, Successful scale-up performance of a novel papaya-clay combo adsorbent: up-flow adsorption of a basic dye, Desalin. Water Treat. (2014) (In press) http://dx.doi.org/10.1080/19443994.2014.944572
[35] S.K. Choi, S. Kim, S.K. Lim, H. Park, Photocatalytic comparison of TiO_2 nanoparticles and electrospun TiO_2 nanofibers: effect of mesoporosity and interparticle charge transfer, J. Phys. Chem. C 114 (2010) 16475–16480.
[36] Y.S. Ho, G. McKay, Pseudo-second order model for sorption processes, Process Biochem. 34 (1999) 451–465.
[37] S. Lagergren, Zur theorie der sogenannten adsorption geloster stoffe, Kungliga SVenska Vetenskapsakademiens, Handlingar Band 24 (1898) 1–39.
[38] C. Sutherland, C. Venkobachar, A diffusion-chemisorption model for simulating biosorption using forest, formes fasciatus, Int. Res. J. Plant Sci. 1 (4) (2010) 107–117.
[39] E.I. Unuabonah, B.I. Olu-Owolabi, A. Taubert, E.B. Omolehin, K.O. Adebowale, SAPK: a novel composite resin for water treatment with very high Zn^{2+}, Cd^{2+}, and Pb^{2+} adsorption capacity, Ind. Eng. Chem. Res. 52 (2) (2013) 578–585.
[40] W.J. Weber Jr, J.C. Morris, Kinetics of adsorption on carbon from solution, J. Sanitary Eng. ASCE 89 (1963) 31–59.
[41] C.-J. Li, G.-R. Xu, B. Zhang, J.R. Gong, High selectivity in visible-light-driven partial photocatalytic oxidation of benzyl alcohol into benzaldehyde over single-crystalline rutile TiO_2 nanorods, Appl. Cat. B Environ. 115–116 (2012) 201–208.
[42] M.M. Montazer-Rahmati, P. Rabbani, A. Abdolali, A.R. Keshtkar, Kinetics and equilibrium studies on biosorption of cadmium lead, and nickel ions from aqueous solutions by intact and chemically modified brown algae, J. Hazard. Mater. 185 (2011) 401–407.
[43] A.A. Ismail, Mesoporous PdO–TiO_2 nanocomposites with enhanced photocatalytic activity, Appl. Cat. B Environ. 117 (2012) 67–72.
[44] E. Kumar, A. Bhatnagar, M. Ji, W. Jung, S.-H. Lee, S.-J. Kim, G. Lee, H. Song, J.Y. Choi, J.S. Yang, B.H. Jeon, Defluoridation from aqueous solutions by granular ferric hydroxide (GFH), Water Res. 43 (2) (2009) 490–498.
[45] M. Sen, M.G. Dastidar, Adsorption–desorption studies on Cr(VI) using non-living fungal biomass, Asian J. Chem. 22 (2010) 2331–2338.
[46] I. Ullah, R. Nadeem, M. Iqbal, Q. Manzoor, Biosorption of chromium onto native and immobilized sugarcane bagasse waste biomass, Ecol. Eng. 60 (2013) 99–107.